Decay mechanisms of ensemble averages of nonlinear oscillators

C. Gong,[1,2] J. Bryan,[1] Q. Su,[1] and R. Grobe[1]

[1]*Intense Laser Physics Theory Unit and Department of Physics, Illinois State University, Normal, Illinois 61790-4560, USA*

[2]*State Key Laboratory for GeoMechanics and Deep Underground Engineering, China University of Mining and Technology, Beijing 100083, China*

(Received 3 November 2021; revised 7 March 2022; accepted 28 April 2022; published xxxxxxxxxx)

The ensemble average of noninteracting particles in a nonlinear oscillator system is investigated. Depending on the initial phase-space distribution, the nonlinearity-induced dephasing mechanism can lead to temporal decays of the average particle position that can be quite different from the standard exponential decay. In fact, the approach to the equilibrium can be Gaussian or even nonmonotonic in time. In the long-time limit, it is possible to construct a single differential equation for the time evolution of the average position. Unlike the infinite set of coupled nonlinear differential equations derived from the standard approach based on the Liouville equation, this equation can be even linear. We also show that the predicted dephasing mechanisms have their direct counterpart in the corresponding dynamics of quantum mechanical wave packets.

DOI: 10.1103/PhysRevA.00.002200

I. INTRODUCTION

While the time evolution of expectation values of quantum mechanical single-particle systems can rarely be predicted by a single particle orbit associated with the classical mechanical limit, the corresponding averages of classical mechanical ensembles are more useful as they reveal a much closer connection to quantum mechanics. For example, the average position of a suitable classical mechanical ensemble follows the quantum expectation value for short times in the chaotic domain and even for longer scales if the dynamics is regular [1]. The classical-quantum discrepancies are most significant at long times, at which the underlying discrete energy structure of the quantum system can become relevant. In this case, the initial collapse associated with dephasing of the states of different energy can even be followed by a quantum mechanical revival, as quasiperiodic quantum states can return arbitrarily close to their initial state [2–4].

The dephasing stage and the approach to equilibrium is an important issue in molecular and atomic spectroscopy [5,6], and in the condensed matter physics of mesoscopic devices. In some cases, it can be associated with a loss of coherence, reflected by the reduction of the off-diagonal elements of a density matrix. The rate of the dephasing process can also provide us with information about the energy level structure in the system. For example, in many-body physics, the dephasing of ensembles of particles can be used as a direct probe of the strength of the interparticle interaction. In most of these examples, the processes are usually characterized by a decay that is exponential in time [7,8]. The most prominent example of such an exponential decay is related to the famous Fermi golden rule.

Recently, the possibility of a temporal Gaussian decay was discussed by Izrailev and co-workers [9,10] in the context of the return probability for closed systems of interacting particles. These authors showed that a new Gaussian decay regime can exist before the usual long-time exponential behavior sets in. Whether exponential or Gaussian dephasing, each decay discussed in the literature so far is characterized by monotonic decreases in time.

In this work, we introduce the possibility of a different class of dephasing mechanisms that can lead even to *nonmonotonic decays*. We demonstrate this for the long-time evolution of the average position of an ensemble of noninteracting particles in a nonlinear (quartic) oscillator potential. To provide three examples, if the initial positions of the particles are Lorentzian distributed, we reproduce the usual exponential decay. However, if this distribution is Gaussian we observe a Gaussian decay, and if the particles are distributed uniformly over a certain range, the decay can be characterized by a series of partial revivals. In fact, our proposed theoretical description for these ensemble averages suggests that the nonlinearity provided by a cubic oscillator is sufficiently general to permit nearly any desired type of time decay behavior of the average position if the initial spatial distribution is designed appropriately.

The traditional phase-space method to study the approach to equilibrium is based on the Liouville equation, which, however, leads in this case to an infinite set of coupled differential equations for the moments of products of the position and momentum variables. To compute the average position is practically impossible as any truncation scheme applied to this infinite set leads to large errors and therefore does not present a practical way to progress.

This paper is organized in the following way. In Sec. II, our nonlinear system and its induced dephasing of ensemble average are defined and discussed. In Sec. III, we perform a harmonic decomposition of a representative single orbit of the cubic oscillator. In Sec. IV, an analytical investigation of the long-time behavior of the ensemble-averaged position is

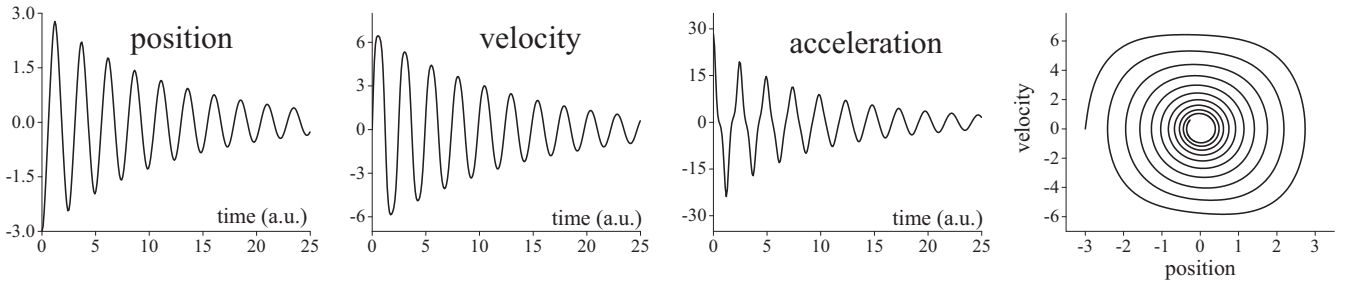

FIG. 1. The time evolution of the (Lorentzian) ensemble's average position $X(t)$, velocity dX/dt, and acceleration d^2X/dt^2, as well as a phase-space portrait $\{X(t),\ dX/dt\}$. We averaged over 20 000 orbits with $X_0 = -3$ and $\Delta X_0 = 0.1$. Each single-particle orbit fulfills $d^2x/dt^2 = -x^3$ with $x(t=0) = x_0$ and $dx/dt(t=0) = 0$.

presented. In Sec. V, we construct differential equations for the ensemble averaged position for the Lorentz initial spatial distribution. In Sec. VI, we suggest that classical mechanical based decay mechanisms have their direct counterpart in the time evolution of quantum mechanical wave packets. Finally in Sec. VII, a summary and outlook into future challenges are presented.

II. NONLINEARLY INDUCED DEPHASING OF ENSEMBLE AVERAGES

It is well known that the frequency of a particle moving in a simple harmonic oscillator potential does not depend on its initial elongation x_0. As a result, in a noninteracting, multiparticle dynamics, all particles take the same time for a round trip along their respective elliptical phase-space orbits. This means that if we introduce spherical coordinates (radius and angle), the corresponding angular speed is identical for any particles. This means they stay "in phase" and the time evolution of the ensemble's average position $X(t)$ is identical to that of a particular single orbit $x(t)$. In this work, we use the lower-case symbol $x(t)$ to denote the position of a single particle and the upper-case symbol $X(t)$ for the corresponding ensemble average of position. Unlike a harmonic potential, if the oscillator's potential energy is quartic, such as $V(x) = x^4/4$, each orbit (initially at rest) has its own (initial position dependent) period $T_{\text{period}}(x_0)$ and the orbits can get out of phase, leading to a nontrivial evolution of $X(t)$, which can be obtained numerically [11–14]. More specifically, we assume that the periodic time evolution of each orbit is governed by $d^2x/dt^2 = -x^3$ with the initial position $x(t=0) = x_0$ and vanishing initial velocity, $dx/dt(t=0) = 0$. Any general prefactor of $-x^3$ can be absorbed into a rescaled time. Due to the nonlinear nature of the cubic restoring force, useful closed-form analytical solutions for the single-particle orbits $x(t; x_0)$ exist but they are complicated as we discuss in Appendix A.

The average position $X(t)$ can be obtained from the single-particle orbits $x(t; x_0)$ as

$$X(t) = \int dx_0\, \rho(x_0)\, x(t; x_0), \tag{2.1}$$

where $\rho(x_0)$ denotes the probability distribution of the set of initial positions x_0. The numerical data for $X(t)$ were obtained as an average of several ten thousand individual orbits, whose initial positions were Lorentz distributed according to $\rho_{\text{L}}(x_0) \equiv (\pi\,\Delta X_0)^{-1}/[1 + (x_0 - X_0)^2/\Delta X_0^2]$, which is centered around a given average position X_0 with a spatial width ΔX_0.

To the best of our knowledge, the only systematic way to derive the equations of motion for $X(t)$ is based on the classical mechanical Liouville equation for the underlying phase-space density. As we show in Appendix B, the solution for $X(t)$ is governed here by an infinite coupled set of first-order differential equations for the average values of all products of the position and the momentum. However, these coupled equations would require a truncation to be numerically feasible. We have shown in Appendix B that these truncation schemes distort the actual solution $X(t)$ significantly as the resulting equation cannot even predict the short-time behavior [associated with only the first few oscillation cycles of $X(t)$] reliably.

To obtain $X(t)$ for all times, we have therefore solved the differential equation for each initial condition x_0 numerically and then used the integral in Eq. (2.1) to average over all solutions to compute $X(t)$. In Fig. 1 we display a typical example for the initial average $X_0 = -3$ and width $\Delta X_0 = 0.1$.

As the orbits get out of phase with each other, the resulting amplitude of the average position $X(t)$ decays in time. However, it is important to note that this decay is entirely different from that of any damped single orbit solution, which would be described by $d^2x/dt^2 = -x^3 - \kappa\, dx/dt$. In this equation, the period would increase significantly as the particle motion slows down. In contrast, Fig. 1 clearly suggests that the period in the decaying function $X(t)$ remains the same for all times. The nonharmonic and nontrivial nature of the average $X(t)$ becomes most apparent in its second derivative d^2X/dt^2 as shown in the figure. During the first early time oscillations its structure is rather different from the long-time behavior, which appears to become more (modulated) sinusoidal. The early time nonharmonic nature is also apparent in the square-like shape of the parametric orbit in $(X, dX/dt)$ phase space, which approaches an inward elliptical spiral only for long times.

III. HARMONIC DECOMPOSITION OF A SINGLE ORBIT OF THE CUBIC OSCILLATOR

While the complicated expressions for the orbits $x(t;\ x_0,\ p_0)$ of the cubic oscillator of Appendix A cannot provide any new intuitive insight into the solution structure or the amount of deviation from sinusoidal solutions, it offers

an alternative algorithm to the direct numerical solution integration technique for differential equations.

We will show in this section that the periodicity of the solution permits us to obtain a rather rapidly converging expansion. In order to follow a more systematic approach where the error can be directly controlled, we can use a harmonic expansion, which is suggested by the periodic nature of the orbits $x(t;\ x_0,\ p_0)$,

$$x(t;\,x_0,\,p_0) = \Sigma_n[A_n(x_0,\,p_0)\sin(n\,\omega\,t) + B_n(x_0,\,p_0)\cos(n\,\omega\,t)], \tag{3.1}$$

where the coefficients follow from the Fourier integrals $A_n \equiv (2/T)\int_0^T dt\ x(t;\ x_0,\ p_0)\ \sin(n\,\omega t)$ and $B_n \equiv (2/T)\int_0^T dt\ x(t;\ x_0,\ p_0)\ \cos(n\,\omega t)$. The period of any orbit with energy $E \equiv p_0^2/2 + x_0^4/4$ is given by $T = 2\int_{-x_m}^{x_m} dx[2(E - x^4/4)]^{-1/2}$, where the maximum elongation is $x_m \equiv (4E)^{1/4}$. The energy dependence of the corresponding frequency $\omega \equiv 2\pi/T$ follows as $\omega(E) = 1.19814E^{1/4}$ as shown in Appendix A.

If we introduce the phase-space angle θ, then $x_0 \equiv (4E)^{1/4}\ \cos(\theta)^{1/2}$ and $p_0 \equiv (2E)^{1/2}\ \sin(\theta)$, all expansion coefficients have the same universal energy dependence and we obtain the expansion

$$x(t;\,x_0,\,p_0) = E^{1/4}\Sigma_{n=\text{odd}}[a_n(\theta)\ \sin(n\omega\,t) + b_n(\theta)\ \cos(n\omega t)]. \tag{3.2}$$

This can lead to a significant simplification if either x_0 or p_0 vanishes. For example, for $x_0 = 0$, corresponding to $\theta = \pi/2$, we can solve $d^2x/dt^2 = -x^3$ numerically and derive from the Fourier integrals the expressions for the lowest-order coefficients $a_1(\pi/2) = 1.350\,58$, $a_3(\pi/2) = -6.088\,11 \times 10^{-2}$, $a_5(\pi/2) = 2.631\,14 \times 10^{-3}$ and $a_7(\pi/2) = -1.165\,34 \times 10^{-4}$, while all $b_n(\pi/2)$ vanish. Similarly, for $p_0 = 0$, corresponding to $\theta = 0$, we find a remarkable symmetry. Here all $a_n(0)$ vanish and $b_1(0) = a_1(\pi/2)$, $b_3(0) = -a_3(\pi/2)$, $b_5(0) = a_5(\pi/2)$, and $b_7(0) = -a_7(\pi/2)$. The coefficients therefore fall off rather rapidly with increasing order, which suggests that the lowest-order approximation for $x(t;x_0,p_0) \approx E^{1/4}[a_1(\theta)\ \sin(\omega t) + b_1(\theta)\ \cos(\omega t)]$ is qualitatively not so bad.

In the case of $p_0 = 0$, we can therefore model each single-particle trajectory approximately by its first few terms in the harmonic expansion,

$$x(t;\,x_0) = 2^{-1/2}x_0[b_1\cos(\omega t) + b_3\cos(3\omega t) + b_5\cos(5\omega t) + \cdots] \tag{3.3}$$

with $b_1 = 1.350\,58$, $b_3 = 6.088\,11 \times 10^{-2}$, and $b_5 = 2.631\,14 \times 10^{-3}$. Here the frequency $\omega = \omega(x_0)$ is a function of the initial position x_0; see the discussion above. The coefficients fall off rather rapidly with increasing order, which suggests that an approximation to $x(t)$ based on only the lowest three terms might be sufficient. For example, for the initial condition $t = 0$ we obtain $x(t = 0;x_0) \approx 2^{-1/2}x_0(b_1 + b_3 + b_5) = 0.999\,914x_0$, which is excellent compared to the exact value x_0.

If we insert the expansion (3.3) for each single orbit into Eq. (2.1) based on Lorentz distribution $\rho(x_0)$, we obtain for the position average $X(t)$ the following expression:

$$\begin{aligned} X(t) &= \int dx_0\,\rho(x_0)\,x(t;x_0) \\ &= \int dx_0\,\rho(x_0)\,2^{-1/2}x_0[b_1\cos(\omega t) + b_3\cos(3\omega t) \\ &\quad + b_5\cos(5\omega t) + \cdots] \\ &= X_0\,2^{-1/2}\{b_1\exp(-\Gamma t)\ [\cos(\Omega t) + \Gamma\sin(\Omega t)/\Omega] \\ &\quad + b_3\exp(-3\Gamma t)[\cos(3\Omega t) + \Gamma\sin(3\Omega t)/\Omega] \\ &\quad + b_5\exp(-5\Gamma t)[\cos(5\Omega t) + \Gamma\sin(5\Omega t)/\Omega] \\ &\quad + \cdots\}. \end{aligned} \tag{3.4}$$

Note that for a cubic oscillator (see Appendix A) the frequency $\omega(x_0) = 2\pi/T_{\text{period}} = \Theta\,x_0$ happens to be just a linear function of the initial elongation x_0, where $\Theta \equiv 0.8472$. This relationship permits us to perform the integration over all positions x_0. In Eq. (3.4) we have also introduced the decay constant $\Gamma \equiv \Theta\Delta X_0$, which depends linearly on the initial spatial width ΔX_0 of the ensemble. The central frequency of $X(t)$, defined here as $\Omega \equiv \Theta|X_0|$, is related to the initial average position of the ensemble.

IV. ANALYTICAL ANALYSIS OF THE LONG-TIME BEHAVIOR OF $X(t)$ AND NONMONOTONIC DECAYS

Higher order terms in Eq. (3.4) decay faster than the first term. As a result, in the long-time limit only the first term survives. Using this fact, we can consider the long-time behavior of the ensemble average position of *arbitrary* initial position distribution $\rho(x_0)$. Using the substitution $\omega \equiv \Theta\,x_0$, we can replace the integration over the (weighted) initial positions x_0 by the frequency integral $X(t) = \Theta^{-2}\int d\omega\,\omega\rho(x_0 = \omega\Theta^{-1})2^{-1/2}b_1\,\cos(\omega\,t)$, which then can be re-expressed as

$$X(t) = 2^{-1/2}b_1\Theta^{-2}d/dt \times \text{Im}\left\{\int d\omega\rho(x_0 = \omega\Theta^{-1})\exp(i\omega t)\right\}. \tag{4.1}$$

This form suggests that the ensemble's approximate time evolution of $X(t)$ is directly related to the time derivative of the imaginary part of the Fourier transformation of the probability distribution of the initial positions. Equation (4.1) provides a unique one-to-one mapping of the initial density $\rho(x_0)$ to the resulting decay of $X(t)$. This relationship might be even (within some mathematical constraints) fully reversible. This means that each $\rho(x_0)$ has its own unique dephasing mechanism. This result allows us to study various interesting decay patterns in more generality. For example, let us examine the decay law associated with the three frequently used probability densities given by Lorentz, Gaussian, and uniform distributions. Each is centered around the average position X_0 and has a spatial width proportional to ΔX_0,

$$\rho_L(x_0) \equiv (1/\pi)\Delta X_0^{-1}/\left[1 + (x_0 - X_0)^2/\Delta X_0^2\right], \tag{4.2a}$$

$$\rho_G(x_0) \equiv (2\pi)^{-1/2}\Delta X_0^{-1}\exp\left[-(x_0 - X_0)^2/(2\Delta X_0)^2\right], \tag{4.2b}$$

$$\rho_U(x_0) \equiv (2\Delta X_0)^{-1}\theta(x_0 - \Delta X_0)\theta(x_0 + \Delta X_0), \tag{4.2c}$$

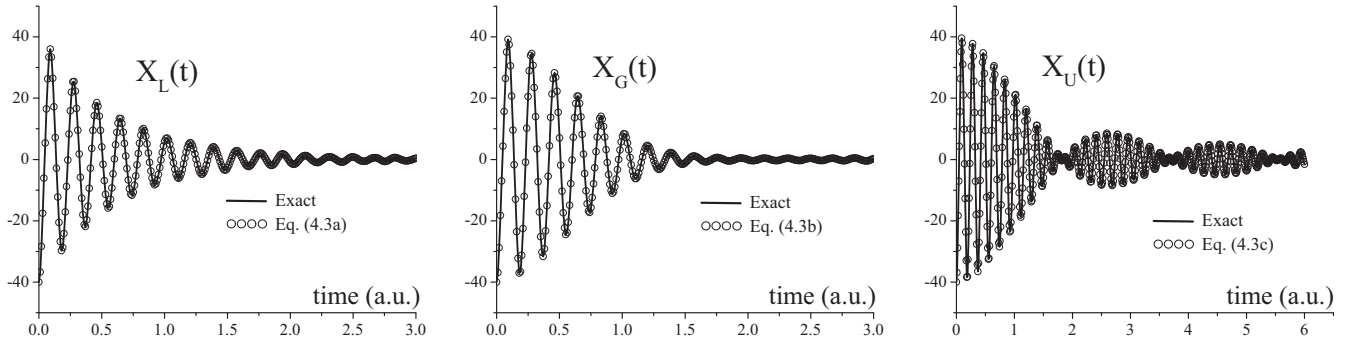

FIG. 2. Comparison of the time evolution of the approximate ensemble averages $X_{\rm L}(t)$, $X_{\rm G}(t)$ and $X_{\rm U}(t)$ with the exact averages over 10 000 orbits of the cubic nonlinear oscillator, where $X_0 = -40$ and $\Delta X_0 = 2$.

where $\theta(x) \equiv x/|x| + 1$ denotes the Heaviside unit-step function. For each case, the corresponding integral (4.1) can be performed fully analytically, leading to the following three decay laws:

$$X_L(t) = X_0 \exp(-\Gamma t)[\cos(\Omega t) + \Gamma \sin(\Omega t)/\Omega], \tag{4.3a}$$

$$X_G(t) = \exp(-\Gamma^2 t^2/2)[X_0 \cos(\Omega t) - t\ \Gamma^2/\Theta \sin(\Omega t)], \tag{4.3b}$$

$$X_U(t) = X_0\, \mathrm{sinc}(\Gamma t)\,[\cos(\Omega t) - \mathrm{sinc}(\Omega t)] + X_0\, \mathrm{sinc}(\Omega t)\cos(\Gamma t), \tag{4.3c}$$

where $\mathrm{sinc}(x) \equiv \sin(x)/x$ and where again the decay constant is $\Gamma \equiv \Theta \Delta X_0$ and the central frequency is $\Omega \equiv \Theta X_0$.

In general, the usual inverse scaling relationship between the variances of the frequency and temporal distributions suggests that an increasing frequency width (measured by the spatial width ΔX_0) leads to a decreasing temporal width (measured by the inverse of the decay constant Γ). This suggests the proportionality $\Gamma \sim \Delta X_0$ for any general initial distribution $\rho(x_0)$. For the three specific examples discussed, we found consistently for the decay constant $\Gamma = 0.8472 \Delta X_0$.

To examine the accuracy of these predictions, in Fig. 2 we have compared the approximate solutions $X_{\rm L}(t)$, $X_{\rm G}(t)$ and $X_{\rm U}(t)$ with the exact ensemble averages over the true orbits associated with the quartic potential $V(x) = x^4/4$. The agreement even for shorter times is quite impressive.

While most decay processes based on various dephasing mechanisms follow an exponential decay, we see that depending on the initial distribution of the positions, also a more rapid *Gaussian decay* process is possible. While Gaussian distributions for all kinds of random variables are routinely being studied, to the best of our knowledge, the possibility of a *temporal* Gaussian decay has been considered only twice in the literature [9,10]. The most interesting decay form, however, occurs for initially uniformly distributed positions. Here the dephasing of all particles leads to a *nonmonotonic decay* that is characterized by periodic reversals.

It is rather interesting that an irreversible dephasing mechanism based on a continuous distribution of particles can lead in some cases even to a *nonmonotonic* decay law for the decaying envelope function of $X(t)$. It is certainly well known that in quantum mechanical systems collapses can be accompanied with revivals [5,6], which are a direct consequence of the underlying discrete energy level structures of some quantum systems. However, in our classical mechanical system there is no discreteness as we have a continuous distribution of all time scales, each given by $T_{\rm period} = 7.416\,298\,71 x_0^{-1}$. The asymptotic long-time behavior of $X_{\rm U}(t)$ in Eq. (4.3c) is given by $X_{\rm U}(t) = X_0\ \mathrm{sinc}(\sigma t)\ \cos(\lambda t)$, where $\sigma \equiv \min(\Gamma, \Omega)$ and $\lambda \equiv \max(\Gamma, \Omega)$. This means that the characteristic revival times occur with a period of $2\pi/\sigma$. This characteristic time scale for $\rho_{\rm U}(x_0)$ is entirely different from the Poincaré reversal time, which would characterize the dynamics if the number of orbits was chosen finite [15].

V. DIFFERENTIAL EQUATIONS FOR THE LORENTZ DISTRIBUTED INITIAL CONDITIONS

Let us examine the Lorentz initial condition in more detail. As the orbit $\{x(t), v(t)\}$ shown in Fig. 1 does not cross itself, X and dX/dt could be considered as phase-space variables, whose evolution might be describable by two first-order differential equations. We therefore feel motivated to search for differential equations that could describe the long-time behavior of $X(t)$.

Equation (3.4) predicts that the exponential decay rates increase linearly with the increasing (odd) order of the harmonics of Ω. This suggests that the long-time behavior is described by just the first two terms that are proportional to b_1. This long-time function, proportional to $\exp(-\Gamma t)[\cos(\Omega t) + \Gamma\ \sin(\Omega t)/\Omega]$, fulfills the second-order differential equation of a simple linearly damped harmonic oscillator,

$$d^2X/dt^2 = -2\Gamma\, dX/dt - (\Gamma^2 + \Omega^2)X. \tag{5.1}$$

If we include the third-order harmonic term with frequency 3Ω in $X(t)$ of Eq. (3.4), then this solution is the sum of the orbits of two harmonic oscillators with frequencies Ω and 3Ω and dissipation rates Γ and 3Γ, respectively. While this seems to be just a linear superposition of two solutions, $X(t)$ no longer satisfies a second-order differential equation. However, one can derive that $X(t)$ satisfies a fourth-order differential equation, which is (surprisingly) again linear. It takes the form

$$d^4X/dt^4 = -8\Gamma dX^3/dt^3 - 2(11\Gamma^2 + 5\Omega^2)dX^2/dt^2 - 24(\Gamma^2 + \Omega^2)\Gamma dX/dt - 9\,(\Gamma^2 + \Omega^2)^2 X. \tag{5.2}$$

Its structure is obviously richer than the simple generalization of Eq. (5.1), which is not even unique and, for

example, could also read $d^4X/dt^4 = -2\Gamma dX^3/dt^3 - (\Gamma^2 + \Omega^2)\, dX^2/dt^2$.

The rather slow fall off of the Lorentzian density $\rho_{\rm L}(x_0)$ with increasing $|x_0|$ leads to the interesting fact about a discontinuity in the second derivative of $X(t)$. In fact, the initial average acceleration $d^2X/dt^2(t=0) = \int dx_0 \rho(x_0) d^2x/dt^2(t=0;x_0) = -\int dx_0 \rho(x_0) x_0^3$ is not finite. This means that one cannot use $t=0$ as an initial condition for the fourth-order differential equation (5.2). However, this is not a contradiction as this equation is valid anyway only in the long-time limit when d^2X/dt^2 is finite.

As a last point, we should remark that the observation that a simple second-order differential equation can govern the long-time ensemble dynamics is not at all obvious or even expected. Let us illustrate this for an ensemble of N different *linear* oscillators, whose positions are governed by Hooke's law $d^2x_{\rm j}/dt^2 = -\Omega_{\rm j}^2 x_{\rm j}$ with $j = 1,\ 2, \ldots, N$. While for $N=1$, a single differential equation is trivially sufficient to describe the average position $X(t) \equiv x_1(t)$, for the $N=2$ system, the position $X(t) \equiv [x_1(t) + x_2(t)]/2$ requires already a fourth-order equation. In order to derive the equation for the N-oscillator average $X(t) \equiv N^{-1}\Sigma_{\rm j}^{\rm N} x_{\rm j}(t)$ for a general N, we can first construct the set of N linear differential equations for $M = 0, 2, 4, \ldots, 2N-2$,

$$d^M X/dt^M = N^{-1}\Sigma_j^N \left(-\Omega_j{}^2\right)^{M/2} x_j, \tag{5.3}$$

where we have used the corresponding equations for each oscillator $\Sigma_{\rm j}^{\rm N} d^{\rm M}x_{\rm j}/dt^{\rm M} = \Sigma_{\rm j}^{\rm N}(-\Omega_{\rm j}^2)^{\rm M/2} x_{\rm j}$. These N equations are obviously linear in $x_{\rm j}$ and therefore they can be inverted to construct each of the N orbits $x_{\rm j}(t)$ in terms of all even-order derivatives of X up to the $(2N-2)$th order. We would then obtain $x_j = f_j(X,\ d^2X/dt^2,\ d^4X/dt^4,\ \ldots,\ d^{2\rm M}X/dt^{2\rm M})$. If we insert these expressions for $x_{\rm j}$ back into the right-hand side of the single $2N$th order differential equation $d^{2\rm N}X/dt^{2\rm N} = N^{-1}\Sigma_{\rm j}^{\rm N}(-\Omega_{\rm j}^2)^{\rm N} x_{\rm j}$ we obtain

$$d^{2N}X/dt^{2N} = N^{-1}\Sigma_j^N \left(-\Omega_j^2\right)^N f_j(X,\ d^2X/dt^2, d^4X/dt^4, \ldots, d^{2N-2}X/dt^{2N-2}). \tag{5.4}$$

This final expression shows that the time evolution of the average position of this N-particle system is governed by a linear differential equation of order $2N-2$. Quite interestingly, this would suggest that in the limit of infinite numbers N a governing differential equation would have to be of infinite order and therefore cannot be found. However, quite remarkably, in the (continuum) limit of infinitely many oscillators ($N \to \infty$), as we have shown in this section, the *long-time behavior* can actually be described by a single equation of just second order; see Eq. (5.1).

Traditionally, nonlinear dynamical systems can be analyzed by a Liouville equation approach in phase space as we outlined in Appendix B. However, due to the nonlinearity, the differential equation for the position average is coupled to all moments of products for space and momentum. This leads to an infinite set of coupled first-order but nonlinear equations. A truncation of the infinite set of equations has not been found possible and any truncation for computational sake, as illustrated in Appendix B, has proven to be completely inadequate. In fact, not even a single oscillation of $X(t)$ can be recovered before it diverges away from the true solution.

VI. QUANTUM MECHANICAL COUNTERPART OF THE DEPHASING MECHANISM

In this section, we will briefly sketch a suggestion for future studies about the question of whether the various decay patterns (predicted from the classical mechanical analysis) have any qualitative counterpart in quantum mechanics. To do so, we have to solve the time-dependent Schrödinger equation of an initial quantum wave packet in the oscillator potential $V(x)$ and examine the time evolution of the expectation value of its position.

In atomic units and in one spatial dimension, the time evolution of the initial quantum wave function $\Psi(x, t=0)$ is determined by $i\partial\Psi(x,t)/\partial t = -(1/2)\partial^2\Psi(x,t)/\partial x^2 + V(x)\Psi(x,t)$. In general, it is not possible to uniquely construct a wave function $\Psi(x, t=0)$ from a classical ensemble phase-space density $\rho(x,p) = \rho_{\rm x}(x)\rho_{\rm p}(p)$. In our case, discussed above, we had $\rho_{\rm p}(p) = \delta(p-0)$, representing all particles to be initially at rest. To establish the relationship to the initial spatial distributions of the classical ensembles of Eqs. (4.2), we have used the three initial wave functions $\Psi_{\rm L}(x, t=0) \equiv \rho_{\rm L}(x)^{1/2}$, $\Psi_{\rm G}(x,\ t=0) \equiv \rho_{\rm G}(x)^{1/2}$ and $\Psi_{\rm U}(x,\ t=0) \equiv \rho_{\rm U}(x)^{1/2}$. These particular choices naturally guarantee that the spatial probability $|\Psi(x, t=0)|^2$ matches initially exactly the corresponding density $\rho_x(x)$ of the corresponding classical ensemble. As $\Psi(x, t=0)$ was chosen real, the initial momentum expectation value vanishes, $\langle p\rangle(t=0) = 0$, corresponding to a quantum particle at rest. However, the associated momentum distribution $|\phi(p,t)|^2$ with $\phi(p,t) \equiv (2\pi)^{-1/2}\int dx\ \exp(-ipx)\ \Psi(x,t)$ has a nonzero width $\langle\Delta p\rangle \neq 0$, which is different from the classical distribution, where we assumed that all particles were initially at rest. This nonvanishing momentum variance is, of course, unavoidable due to the Heisenberg uncertainty principle as the position variance $\langle\Delta x\rangle(t=0) = \Delta X_0$ was not infinite.

Before we discuss the nonlinearity induced irreversible decay for $V(x) = x^4/4$, we summarize the linear case for $V(x) = x^2/2$. Here for any initial quantum mechanical wave function, the quantum expectation value $\langle x\rangle(t)$ remains oscillatory and does not decay. In fact, it is identical to the classical ensemble average at all times.

In Fig. 3 we have graphed the time evolution of the quantum expectation value of the position $\langle x\rangle(t) \equiv \int dx \Psi^*(x,t) x \Psi(x,t)$ for the three different initial wave functions for the nonlinear potential $V(x) = x^4/4$.

Fully consistent with the predictions of the classical mechanical ensemble, we find also here that the spatially Gaussian quantum distribution leads to a temporally Gaussian decay of the position's envelope and the Lorentzian-like distributed wave function leads to an exponential decay. It is quite remarkable that even the revival-based predictions for $\rho_{\rm U}(x)$ find in the wave function $\Psi_{\rm U}(x,t)$ their direct quantum mechanical counterpart. Obviously, the nonvanishing momentum variance $\langle\Delta p\rangle(t=0)$ could add another dephasing mechanism that might contribute to the overall decay, but at least for our chosen sets of initial conditions for $X_0 = -10$ and $\Delta X_0 = 0.5$, the agreement with the analytical expressions Eqs. (4.3) that were derived for the classical mechanical ensemble averages is still superb.

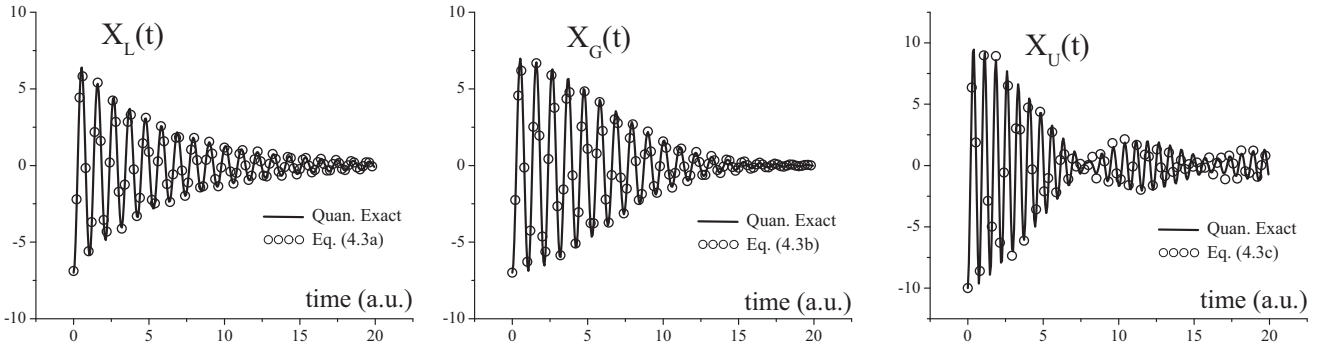

FIG. 3. Comparison of the time evolution of the quantum mechanical average values $X(t) \equiv \langle x \rangle(t)$ with the analytical expressions Eqs. (4.3), which are based on classical mechanical ensemble averages. The initial wave functions were chosen to be $\Psi(x, t = 0) = \rho(x)^{1/2}$ with the corresponding densities of Eq. (4.2). The Schrödinger equation was solved on a 9000×300 space-time grid with equidistant spacings $\Delta x = 0.0033$ and $\Delta t = 0.066$. The initial densities were Lorentzian $\rho_{\rm L}(x)$ from Eq. (4.2a) with $X_0 = -7$ and $\Delta X_0 = 0.2$, Gaussian $\rho_{\rm G}(x)$ (4.2b) with $X_0 = -7$ and $\Delta X_0 = 0.2$, and uniform $\rho_{\rm U}(x)$ (4.2c) with $X_0 = -10$ and $\Delta X_0 = 0.5$.

As a last comment, we note that, due the noncommutativity of the position and momentum quantum operators, the corresponding Heisenberg equations of motion for the expectation values $\langle x^{\rm n} p^{\rm m} \rangle$ are in principle different than those equations derived in Appendix B based on the classical mechanical Liouville equation. But apparently, these differences do not affect the time evolution of $\langle x \rangle$ too much.

VII. SUMMARY AND OUTLOOK INTO FUTURE CHALLENGES

In the present work, we have discussed the decay mechanisms based on the dephasing of ensembles of single orbits with different frequencies each. We suggest that in the long-time limit, it is possible to design the initial distribution in a way to produce a wide variety of temporal decay behaviors for the ensemble-averaged position beyond the usual exponential decay. To be concrete, we have focused our attention on individual orbits in a quartic potential. However, the main conclusions obtained here can be generalized to other classes of nonlinear oscillators as well. Our analysis has relied on the periodicity of the average position as well as the knowledge about how the local frequency depends on each particle's turning point coordinate.

To better understand the dynamics under which mechanisms are nonlinear classical as well as which quantum systems can relax into their steady states is, of course, of wide interest to the atomic and molecular physics communities. In our example, we have also assumed that particles do not interact with each other, apart from their interactions with the potential. The possibility of an interparticle interaction will likely present an additional challenge, which would certainly be of interest also to the many-body particle physics community. We have also assumed that each orbit is in an isolated environment. It might be interesting to observe how the inclusion of dissipative mechanisms on each orbit would affect the global dephasing behavior.

The present investigation has been completely based on a classical mechanical analysis. If, in addition, the internal energy spectrum needs to be considered as discrete, the finite energy spacing in that case will serve as an additional degree of freedom in how the ensemble average may vary in time.

The excellent agreement between the classical mechanical and quantum mechanical wave packet calculations suggests that the various aspects of the newly predicted decay patterns can possibly also have experimental implications. For example, using suitable tuned and tailored laser pulses, it has become possible to prepare electronic (as well as vibrational) states in atoms and molecules as spatially localized wave packets. For example, following some theoretical suggestions [16,17], the pioneering experimental work by the Stroud group [18] created wave packets in sodium atoms. Here the electron was localized by exciting a stationary extreme Stark state from the $n = 30$ manifold in a DC electric field followed by the application of a terahertz electromagnetic half-cycle pulse. While the resulting classicallike orbit was governed here by the nonlinearity of the Coulomb potential, the nonlinear dephasing mechanism of this initially localized wave packet could be described by a similar approach as outlined in the present work. All these are interesting questions to be further investigated.

ACKNOWLEDGMENTS

C.G. would like to thank ILP for the nice hospitality during his visit to Illinois State University and acknowledges the China Scholarship Council program for his Ph.D. research. This work has been supported by the NSF PHY-2106585 and Research Corporation and the National Natural Science Foundation of China (NSFC) under Grant No. 11974419.

APPENDIX A: ANALYTICAL ANALYSIS FOR A SINGLE ORBIT OF THE CUBIC OSCILLATOR

The solutions to the equation, $d^2x/dt^2 = -x^3$ with the initial conditions $x(t = 0) = x_0$ and $p(t = 0) = dx/dt(t = 0) = p_0$ can be expressed [19] in terms of the complicated Jacobi elliptic sine function $\mathrm{Jsn}(x)$ with parameter -1. This meromorphic and periodic function oscillates between -1 and 1 and can be defined as an inverse of an incomplete elliptic integral, such that $\mathrm{Jsn}[u(\alpha)] = \sin(\alpha)$, where $u(\alpha) \equiv \int_0^\alpha d\tau [1 + \sin^2(\tau)]^{-1/2}$. The exact solution is

$$x(t; x_0, p_0) = se\, 2^{1/2}\, \mathrm{Jsn}(et + \phi), \tag{A1}$$

where $s \equiv p_0/|p_0|$ is just a sign factor, the "scaled frequency" $e \equiv E^{1/4} \equiv [p_0^2/2 + x_0^4/4]^{1/4}$ is related to the energy E, and the "phase" is defined in terms of the inverse Jacobi elliptic function IJsn as $\phi \equiv s\ \mathrm{IJsn}[x_0 2^{-1/2}/e]$ with parameter -1. The occurrence of the sign factor s is not so unusual, as it is also required in the sine solution of the ordinary harmonic oscillator. The amount of the prefactor $e2^{1/2}$ is the maximum amplitude, such that $(e2^{1/2})^4/4 = p_0^2/2 + x_0^4/4$, which follows from energy conservation. The Jacobi function $\mathrm{Jsn}(t)$ has a period of $4E(-1) = 5.24412\ldots$, where $E(t)$ is the complete elliptic integral of the first kind. As we also show in our analysis below, the solution (A1) has therefore a period $T = 5.244/e$ corresponding to a true frequency defined as $\omega(E) \equiv 2\pi/T = 1.1981e$.

When $p_0 = 0$, using energy conservation $(dx/dt)^2/2 + x^{\mathrm{n}}/n = x_0^{\mathrm{n}}/n$, the period of a particle of mass $m = 1$ evolving in any nonlinear binding potential $V(x) = x^{\mathrm{n}}/n$ is given by $T_{\mathrm{period}} = 2(n/2)^{1/2} \int_{-x_0}^{x_0} dx[x_0^{\mathrm{n}} - x^{\mathrm{n}}]^{-1/2}$, which amounts for our case of the quartic potential $(n = 4)$ to $T_{\mathrm{period}} = 7.416\,298\,71 x_0^{-1}$. This means that for this oscillator the frequency $\omega(x_0) = 2\pi/T_{\mathrm{period}} = \Theta x_0$ is just a linear function of the initial elongation x_0, where $\Theta \equiv 0.8472$.

APPENDIX B: LIOUVILLE EQUATION APPROACH

To the best of our knowledge, the only way to derive systematically the governing equations of motions for ensemble averages [20–22] is based on the Liouville equation for the time evolution of the phase-space density $\rho(x, p, t)$. We will illustrate in this appendix that, while this indirect approach for $X(t)$ is in principle exact, it cannot be easily implemented numerically. For an ensemble of classical mutually noninteracting particles of unit mass, the phase-space density $\rho(x, p, t)$ in a potential $V(x)$ follows from the preservation of the local phase-space volume $d\rho/dt = 0$ as

$$\partial\, \rho(x, p, t)/\partial t = -p\, \partial\, \rho(x, p, t)/\partial x + dV(x)/dx\ \partial\, \rho(x, p, t)/\partial p. \quad \text{(B1)}$$

This partial differential equation in t, x, and p allows us to derive the set of governing equations of motion for any ensemble average value, defined as $\langle x^n p^m\rangle(t) \equiv \iint dx dp\, x^n p^m \rho(x, p, t)$ for any integers n and m. Taking first the time derivative of this average value $\langle x^n p^m\rangle$, transferring the derivative to ρ inside the integral, and using integration by parts with regard to x and p, we obtain

$$d\langle x^n p^m\rangle/dt = n\langle x^{n-1} p^{m+1}\rangle - m\langle x^n p^{m-1} dV/dx\rangle. \quad \text{(B2)}$$

This means that for general potentials $V(x)$ that contain higher powers than x^2, each moment is typically coupled to moments of even higher power. For our specific case, where $V(x) = x^4/4$, there is an infinite set of coupled first-order linear differential equations for $\langle x^n p^m\rangle$. For example, the first eight equations that govern the time evolution of $X(t) = \langle x\rangle$ are

$$n = 1, \quad m = 0, \quad dX/dt = \langle p\rangle, \quad \text{(B3a)}$$

$$n = 0, \quad m = 1, \quad d\langle p\rangle/dt = -\langle x^3\rangle, \quad \text{(B3b)}$$

$$n = 3, \quad m = 0, \quad d\langle x^3\rangle/dt = 3\langle x^2 p\rangle, \quad \text{(B3c)}$$

$$n = 2, \quad m = 1, \quad d\langle x^2 p\rangle/dt = 2\langle x p^2\rangle - \langle x^5\rangle, \quad \text{(B3d)}$$

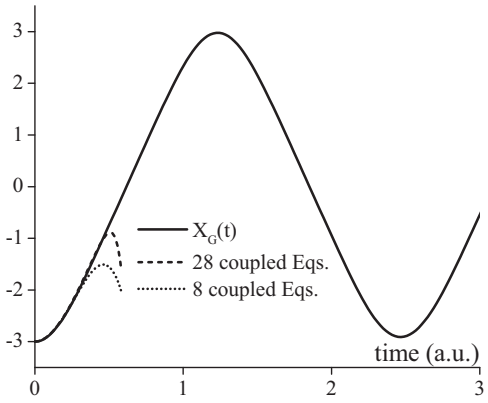

FIG. 4. The time evolution of the ensemble average $X_{\mathrm{G}}(t)$ obtained from the truncated set of coupled eight and 28 first-order differential equations (B3) for $X_0 = -3$ and $\Delta X_0 = 0.1$. It is compared to the exact graph obtained by averaging over 10 000 orbits.

$$n = 1, \quad m = 2, \quad d\langle x p^2\rangle/dt = \langle p^3\rangle - 2\langle x^4 p\rangle, \quad \text{(B3e)}$$

$$n = 5, \quad m = 0, \quad d\langle x^5\rangle/dt = 5\langle x^4 p\rangle, \quad \text{(B3f)}$$

$$n = 0, \quad m = 3, \quad d\langle p^3\rangle/dt = -3\langle x^3 p^2\rangle, \quad \text{(B3g)}$$

$$n = 4, \quad m = 1, \quad d\langle x^4 p\rangle/dt = 4\langle x^3 p^2\rangle - \langle x^7\rangle. \quad \text{(B3h)}$$

While it can be shown that any single differential equation of Nth order is equivalent to N sets of coupled equations of first-order, the reverse is not always true in general. We have not been able to rewrite Eqs. (B3) to construct a single (even just approximate) differential equation for $X(t)$. In addition, the set of Eqs. (B3) is also rather unsuitable for obtaining numerical solutions for $X(t)$. Unfortunately, these eight coupled equations cannot be solved consistently, as this set is not closed and we would need the corresponding equations for $\langle x^3 p^2\rangle$ and $\langle x^7\rangle$. If we were able to find an approximation such that we could replace these two specific moments in terms of functions of the lower moments, then this set would be closed, as is the case for linear and quadratic potentials.

There are some special cases for which these approximations are reasonable, for example if the initial phase-space density is sharp, i.e., $\rho(x, p, t = 0) = \delta(x - X_0)\delta(p - P_0)$, then all initial moments would factorize, i.e., $\langle x^n p^m\rangle(t) \equiv X_0^n(t)\, P_0^m(t)$. In order to evaluate the predictive power of this Liouville-based approach, we have artificially truncated the set of equations by setting the higher-order moments equal to zero. In the first case, we put the right-hand side of Eqs. (B3g) and (B3h) equal to zero, i.e., $d\langle p^3\rangle/dt = d\langle x^4 p^2\rangle/dt = 0$ and solved the resulting closed set of eight equations. In the second case, we assumed that $d\langle x p^6\rangle/dt = d\langle x^5 p^4\rangle/dt = d\langle x^9 p^2\rangle/dt = d\langle x^{13}\rangle/dt = 0$ and solved the 28 coupled equations. In each case, we assumed an initial Gaussian phase-space density $\rho(x, p, t = 0) = \delta(p)\ \Delta X_0^{-1}(2\pi)^{-1/2}\ \exp[-(x - X_0)^2 2^{-1}\Delta X_0^{-2}]$ with $X_0 = -3$ and $\Delta X_0 = 0.1$ to calculate the initial moments. The initial values for the moments $\langle x^{\mathrm{n}} p^{\mathrm{m}}\rangle$ with $m \neq 0$ vanish, while $\langle x^{\mathrm{n}}\rangle$ was computed via $\iint dx dp x^{\mathrm{n}} \rho(x, p)$.

In Fig. 4 we compare the two solutions for $X(t)$ with the exact graph, obtained numerically from the average over 10 000 initially Gaussian distributed orbits. It is clear that with

eight as well as 28 coupled equations, the predictions of the Liouville-based approach fail completely to predict correctly even just the very first quarter cycle of $X(t)$. It might be possible to find some truncation schemes that might accelerate the convergence of these equations, but this challenge is far beyond the scope of this appendix, whose main purpose was to show that this systematic Liouville-based approach to derive a governing equation of motion for $X(t)$ is very problematic for the cubic oscillator.

[1] F. Haake, S. Gnutzmann, and M. Kus, *Quantum Signatures of Chaos*, 4th ed. (Springer, Heidelberg, 2021).

[2] P. Bocchieri and A. Loinger, Phys. Rev. **107**, 337 (1957).

[3] I. C. Percival, J. Math. Phys. **2**, 235 (1961).

[4] L. S. Schulman, Phys. Rev. A **18**, 2379 (1978).

[5] J. H. Eberly, N. B. Narozhny, and J. J. Sanchez-Mondragon, Phys. Rev. Lett. **44**, 1323 (1980).

[6] A. A. Karatsuba and E. A. Karatsuba, J. Phys. A **42**, 195304 (2009).

[7] A. K. Evans and P. V. Coveney, Proc. R. Soc. London, Ser. A **448**, 293 (1995).

[8] D. H. U. Marchetti and W. F. Wreszinski, *Asymptotic Time Decay in Quantum Physics* (World Scientific, New Jersey, 2013).

[9] F. Izrailev and A. Castaneda-Mendoza, Phys. Lett. A **350**, 355 (2006).

[10] V. V. Flambaum and F. M. Izrailev, Phys. Rev. E **61**, 2539 (2000).

[11] G. Duffing (Vieweg, Braunschweig) Heft 41/42 (1918), p. 134.

[12] J. M. T. Thompson and H. B. Stewart, *Nonlinear Dynamics and Chaos* (Wiley, New York, 2002).

[13] I. Kovacic and M. J. Brennan, *The Duffing Equation: Nonlinear Oscillators and their Behavior* (Wiley, New York, 2011).

[14] C. N. McGinnis, D. L. Holland, Q. Su, and R. Grobe, Phys. Rev. E **101**, 032202 (2020).

[15] *XIVth International Congress on Mathematical Physics*, edited by L. Barreira and J. C. Zambrini (World Scientific, Singapore, 2006), p. 415.

[16] Z. D. Gaeta, M. W. Noel, and C. R. Stroud, Jr., Phys. Rev. Lett. **73**, 636 (1994).

[17] I. Bialynicki-Birula, M. Kalinski, and J. H. Eberly, Phys. Rev. Lett. **73**, 1777 (1994).

[18] J. Bromage and C. R. Stroud, Jr., Phys. Rev. Lett. **83**, 4963 (1999).

[19] W. P. Reinhardt and P. L. Walker, in *NIST Digital Library of Mathematical Functions* (National Institute of Standards and Technology), Chap. 22, https://dlmf.nist.gov/22.13.

[20] R. C. Tolman, *The Principles of Statistical Mechanics* (Dover, New York, 1979).

[21] H. J. W. Müller-Kirsten, *Basics of Statistical Physics* (World Scientific, Singapore, 2013).

[22] R. Kubo, J. Math. Phys. **4**, 174 (1963).